6. Tomovic, R., "Sensitivity Analysis of Dynamic Systems," p. 26, McGraw Hill, New York (1963).
7. Wang, F. S. and D. D. Perlmutter, *AIChE J.*, **14**, 335 (1968).
8. ———, Ph.D. thesis, Univ. Illinois, Urbana, (1966).
9. Weiss, L., and E. F. Infante, *Proc. Nat'l Acad. Sci.*, **54**, No. 1, 44 (1965).

Manuscript received May 27, 1967; revision received January 9, 1968; paper accepted January 13, 1968. Paper presented at AIChE New York City meeting.

Dispersion in Developing Velocity Fields

WILLIAM N. GILL, V. ANANTHAKRISHNAN, and RICHARD J. NUNGE

Clarkson College of Technology, Potsdam, New York

Convective diffusion in laminar flows which develop from rest and in the velocity entrance region of tubes, is studied. Criteria for the validity of the simple dispersion model are established by comparison of analytical results with numerical experiments.

It is found that the extent of dispersion is less in developing velocity fields than in those which are fully developed. This occurs because dispersion is enhanced by differences in the velocity of the fluid particles on a plane perpendicular to the main direction of flow. Such differences are greatest when the flow is fully developed.

Previous work on dispersion in well defined systems has been concerned exclusively with fully developed flows which are independent of the axial coordinate (*1* to *3*, *5*, *7* to *11*, *13*). This is so, even though the velocity entrance region is of considerable practical importance (*12*), primarily because of the apparent mathematical difficulty involved in analyzing such systems.

Another effect which may well influence dispersion experiments is the development of the velocity field from rest. It is easy to see that this is the case in the most easily conceived dispersion experiments with slug stimuli. Probably, the simplest possible way to introduce a slug of fluid into a stream in a well defined manner is to start the system from rest with the slug initially separated from the main body of fluid by partitions on both sides. Indeed it is quite difficult to introduce a well defined slug into a steadily flowing stream without disturbing the flow and distorting the slug. Consequently, it seems desirable to analyze carefully dispersion in flows which start from rest so that the results of such experiments may be interpreted in a completely rational manner. Here, the results of a recent study of dispersion in time variable flow (*8*) are generalized somewhat to provide the basis for performing such an analysis.

It will be shown that the dispersion coefficient is time dependent for time dependent flows and is given explicitly by Equation (22) when the flow develops from rest. Once the dispersion coefficient is known it enables one to predict the average concentration distribution in higher dimensional systems in terms of well known solutions to the one dimensional Equation (9). In so doing, the dispersion model markedly simplifies the theory of convective diffusion.

The purposes of our work in the present article are:

1. to examine analytically the dispersion model for velocity fields in which the components depend on the axial coordinate which is parallel to the main direction of flow as is the case in the velocity entrance region of a tube.

2. to establish approximate limits for the validity of the analytical theory by comparing the results with numerical experiments carried out as finite difference solutions of the convective diffusion equation for the important case of flow in the velocity entrance region of a tube.

3. to examine the effects on dispersion of having the velocity field develop from rest. For this type of time dependent flow we shall determine approximate limits of applicability of the analytical dispersion theory. This will be done also by comparing the analytical theory with finite difference calculations.

ANALYSIS

Consider the velocity field to be prescribed so that $u = u(t, x, r)$ and $v = v(t, x, r)$ are known, continuous functions of time and the spatial coordinates. Consequently the convective diffusion equation in cylindrical coordinates is

$$\frac{\partial c}{\partial t} + u(t,x,r)\frac{\partial c}{\partial x} + v(t,x,r)\frac{\partial c}{\partial r} = \frac{1}{r}\frac{\partial}{\partial r} r\, D_r(t,r)\frac{\partial c}{\partial r} + \frac{\partial}{\partial x} D_x(t,r)\frac{\partial c}{\partial x} \quad (1)$$

Note that we have taken account of turbulence in a phenomenological way by allowing for eddy diffusion in $D_r(t, r)$ and $D_x(t, r)$.

In dimensionless form Equation (1) is

$$\frac{\partial \theta}{\partial \tau} + u_1\frac{\partial \theta}{\partial X} + N_{Pe}\, v_1\frac{\partial \theta}{\partial y} = \frac{1}{y}\frac{\partial}{\partial y} y\, D_1\frac{\partial \theta}{\partial y} + \frac{1}{N_{Pe}^2}\frac{\partial}{\partial X} D_2\frac{\partial \theta}{\partial X} \quad (2)$$

and we shall restrict our attention to boundary conditions of the kind

$$\frac{\partial \theta}{\partial y}(\tau, X, 0) = \frac{\partial \theta}{\partial y}(\tau, X, 1) = 0 \quad (3)$$

The solution of Equation (2) is now formulated as a series expansion in $\partial^k\theta_m/\partial X_1^k$ where X_1 is defined by

$$X_1 = X - \int_0^\tau U(\tau)\,d\tau$$

and

$$U(\tau) = 2\int_0^1 y u_1 dy \quad (4)$$

Then Equation (2) becomes

$$\frac{\partial \theta}{\partial \tau} + (u_1 - U)\frac{\partial \theta}{\partial X_1} + N_{Pe}\, v_1\frac{\partial \theta}{\partial y} = \frac{1}{y}\frac{\partial}{\partial y} y\, D_1\frac{\partial \theta}{\partial y} + \frac{1}{N_{Pe}^2}\frac{\partial}{\partial X_1} D_2\frac{\partial \theta}{\partial X_1} \quad (5)$$

Now let

$$\theta = \theta_m + \sum_{k=1}^{\infty} f_k(\tau, X_1, y)\frac{\partial^k \theta_m}{\partial X_1^k} \quad (6)$$

where

$$\theta_m = 2\int_0^1 y\theta dy$$

If one substitutes Equation (6) into Equation (5) the result is

$$\frac{\partial\theta_m}{\partial\tau}+\sum_{k=1}^{\infty}\left\{\frac{\partial f_k}{\partial\tau}\frac{\partial^k\theta_m}{\partial X_1{}^k}+f_k\frac{\partial^{k+1}\theta_m}{\partial\tau\partial X_1{}^k}\right.$$
$$+(u_1-U)\left[\frac{\partial\theta_m}{\partial X_1}+\frac{\partial f_k}{\partial X_1}\frac{\partial^k\theta_m}{\partial X_1{}^k}+f_k\frac{\partial^{k+1}\theta_m}{\partial X_1{}^{k+1}}\right]$$
$$+N_{Pe}\,v_1\frac{\partial f_k}{\partial y}\frac{\partial^k\theta_m}{\partial X_1{}^k}-\frac{1}{y}\frac{\partial}{\partial y}yD_1\frac{\partial f_k}{\partial y}\frac{\partial^k\theta_m}{\partial X_1{}^k}$$
$$-\frac{D_2}{N_{Pe}{}^2}\left[\frac{\partial^2\theta_m}{\partial X_1{}^2}+\frac{\partial^2 f_k}{\partial X_1{}^2}\frac{\partial^k\theta_m}{\partial X_1{}^k}\right.$$
$$\left.\left.+2\frac{\partial f_k}{\partial X_1}\frac{\partial^{k+1}\theta_m}{\partial X_1{}^{k+1}}+f_k\frac{\partial^{k+2}\theta_m}{\partial X_1{}^{k+2}}\right]\right\}=0 \quad (7)$$

Since

$$\frac{\partial\theta_m}{\partial\tau}=K\frac{\partial^2\theta_m}{\partial X_1{}^2} \quad (8)$$

it follows that

$$\frac{\partial^{k+1}\theta_m}{\partial\tau\partial X_1{}^k}=K\frac{\partial^{k+2}\theta_m}{\partial X_1{}^{k+2}} \quad (9)$$

and therefore Equation (7) becomes

$$\left[\frac{\partial f_1}{\partial\tau}+(u_1-U)\left(1+\frac{\partial f_1}{\partial X_1}\right)+N_{Pe}\,v_1\frac{\partial f_1}{\partial y}\right.$$
$$\left.-\frac{1}{y}\frac{\partial}{\partial y}yD_1\frac{\partial f_1}{\partial y}-\frac{D_2}{N_{Pe}{}^2}\frac{\partial^2 f_1}{\partial X_1{}^2}\right]\frac{\partial\theta_m}{\partial X_1}$$
$$+\left[\frac{\partial f_2}{\partial\tau}+(u_1-U)\left(\frac{\partial f_2}{\partial X_1}+f_1\right)+N_{Pe}\,v_1\frac{\partial f_2}{\partial y}\right.$$
$$-\frac{1}{y}\frac{\partial}{\partial y}yD_1\frac{\partial f_2}{\partial y}-\frac{D_2}{N_{Pe}{}^2}\frac{\partial^2 f_2}{\partial X_1{}^2}$$
$$\left.\left.+\left[K-\frac{D_2}{N_{Pe}{}^2}\left(1+2\frac{\partial f_1}{\partial X_1}\right)\right]\right]\frac{\partial^2\theta_m}{\partial X_1{}^2}$$
$$+\sum_{k=1}^{\infty}\left\{\frac{\partial f_{k+2}}{\partial\tau}+Kf_k+(u_1-U)\left[\frac{\partial f_{k+2}}{\partial X_1}+f_{k+1}\right]\right.$$
$$+N_{Pe}\,v_1\frac{\partial f_{k+2}}{\partial y}-\frac{1}{y}\frac{\partial}{\partial y}yD_1\frac{\partial f_{k+2}}{\partial y}$$
$$\left.-\frac{D_2}{N_{Pe}{}^2}\left[\frac{\partial^2 f_{k+2}}{\partial X_1{}^2}+2\frac{\partial f_{k+1}}{\partial X_1}+f_k\right]\right\}\frac{\partial^{k+2}\theta_m}{\partial X_1{}^{k+2}}=0 \quad (10)$$

If one equates each coefficient of $\partial^k\theta_m/\partial X_1{}^k$ to zero the following system of equations is generated,

$$\frac{\partial f_1}{\partial\tau}+(u_1-U)\frac{\partial f_1}{\partial X_1}+N_{Pe}\,v_1\frac{\partial f_1}{\partial y}$$
$$=\frac{1}{y}\frac{\partial}{\partial y}yD_1\frac{\partial f_1}{\partial y}+\frac{D_2}{N_{Pe}{}^2}\frac{\partial^2 f_1}{\partial X_1{}^2}+(U-u_1) \quad (11a)$$

$$\frac{\partial f_2}{\partial\tau}+(u_1-U)\frac{\partial f_2}{\partial X_1}+N_{Pe}\,v_1\frac{\partial f_2}{\partial y}=\frac{1}{y}\frac{\partial}{\partial y}yD_1\frac{\partial f_2}{\partial y}$$
$$+\frac{D_2}{N_{Pe}{}^2}\frac{\partial^2 f_2}{\partial X_1{}^2}+(U-u_1)f_1$$
$$+\left[\frac{D_2}{N_{Pe}{}^2}\left(1+2\frac{\partial f_1}{\partial X_1}\right)-K\right] \quad (11b)$$

$$\frac{\partial f_{k+2}}{\partial\tau}+(u_1-U)\frac{\partial f_{k+2}}{\partial X_1}+N_{Pe}\,v_1\frac{\partial f_{k+2}}{\partial y}$$
$$=\frac{1}{y}\frac{\partial}{\partial y}yD_1\frac{\partial f_{k+2}}{\partial y}+\frac{D_2}{N_{Pe}{}^2}\frac{\partial^2 f_{k+2}}{\partial X_1{}^2}+\frac{2D_2}{N_{Pe}{}^2}\frac{\partial f_{k+1}}{\partial X_1}$$
$$+(U-u_1)f_{k+1}+\left(\frac{D_2}{N_{Pe}{}^2}-K\right)f_k,\quad k=1,2,\ldots \quad (11c)$$

Superficially, Equations (11) appear to be even more difficult to deal with than Equation (5). However, there is one fundamental difference between Equations (5) and (11) which makes the latter much easier to solve; this is that Equations (11) are inhomogeneous and therefore they have nontrivial solutions which are independent of τ if (u_1-U) is independent of τ. For time dependent flows one can render u_1-U independent of τ, for the purpose of finding a solution, by using the Duhamel theorem (9) as is done below.

The determination of the dispersion coefficient is of central importance in the present analysis. For the purpose of finding the proper expression for K, let us assume for the moment that $f_1(\tau, X, y)$ is known, and then it is necessary to consider the solution of Equation (11b) for f_2. Thus, we return to (τ, X, y) coordinates and let F satisfy

$$\frac{\partial F}{\partial\tau}+u_1\frac{\partial F}{\partial X}+N_{Pe}\,v_1\frac{\partial F}{\partial y}=\frac{1}{y}\frac{\partial}{\partial y}yD_1\frac{\partial F}{\partial y}$$
$$+\frac{D_2}{N_{Pe}{}^2}\frac{\partial^2 F}{\partial X^2}+\frac{D_2}{N_{Pe}{}^2}\left[1+2\frac{\partial f_1}{\partial X}(\lambda,x,y)\right]$$
$$-[u_1(\lambda,x,y)-U(\lambda)]f_1(\lambda,x,y)-K(\lambda) \quad (12)$$

where λ is a constant parameter, and the Duhamel theorem enables one to relate f_2 and F by

$$f_2=\frac{\partial}{\partial\tau}\int_0^{\tau}F(\lambda,\tau-\lambda,X,y)\,d\lambda \quad (13)$$

It is convenient to define another function, G, such that

$$\frac{\partial G}{\partial\tau}+u_1\frac{\partial G}{\partial X}+N_{Pe}\,v_1\frac{\partial G}{\partial y}=\frac{1}{y}\frac{\partial}{\partial y}yD_1\frac{\partial G}{\partial y}$$
$$+\frac{D_2}{N_{Pe}{}^2}\frac{\partial^2 G}{\partial X^2}+\frac{D_2}{N_{Pe}{}^2}\left[1+2\frac{\partial f_1}{\partial X}(\lambda,\sigma,y)\right]$$
$$-[u_1(\lambda,\sigma,y)-U(\lambda)]f_1(\lambda,\sigma,y)-K(\lambda) \quad (14)$$

where

$$F=\frac{\partial}{\partial X}\int_0^{X}G(\lambda,\sigma,\tau,X-\sigma,y)\,d\sigma \quad (15)$$

The difficulty involved in determining K is closely related to the behavior of v_1. For systems where v is independent of X as $X\to\infty$, the difficulty is markedly reduced because the solution for G can be generated by superposition in the form

$$G=G_1(\lambda,\sigma,y)+G_2(\tau,X,y)$$

and K is an eigenvalue which is determined such that $dG_1/dy\ (\lambda,\sigma,1)=0$.

If we consider forced flows between impermeable, rigid, parallel boundaries, then as $X\to\infty$, $u(\tau,X,y)\to u(\tau,y)$ and $v_1(\tau,X,y)\to 0$. In this event, a solution of Equation (14) exists which is valid for large X, and which satisfies

$$\frac{1}{y}\frac{d}{dy}yD_1\frac{dG_\infty}{dy}=[u_1(\lambda,\sigma,y)-U(\lambda)]f_1(\lambda,\sigma,y)$$
$$+K(\lambda)-\frac{D_2}{N_{Pe}{}^2}\left[1+2\frac{\partial f_1}{\partial X}(\lambda,\sigma,y)\right] \quad (16)$$

and

$$\frac{dG_\infty}{dy}(0)=\frac{dG_\infty}{dy}(1)=0 \quad (17)$$

if, and only if,

$$K(\tau)=\frac{2D_2}{N_{Pe}{}^2}\int_0^1 y\left[1+2\frac{\partial f_1}{\partial X}(\tau,X,y)\right]dy$$
$$-2\int_0^1 y(u_1-U)f_1(\tau,X,y)\,dy \quad (18)$$

This is obviously a contradiction since it implies a function of τ is equal to a function of τ and X. It is worthwhile to discuss the reasons for this contradiction. First, note that Equation (9) implies K is a function of τ only.

Second, the X dependence of f_1 is required only because the velocity field depends on X. However, if we restrict attention to regions where u_1 and v_1 do not depend on X, then it is not necessary for f_1 to depend on X and no contradiction arises. If on the other hand we allow K to depend on both τ and X to avoid this contradiction, then, the problem of finding the f_k functions is complicated enormously because they cannot be solved for independently as all the differential equations for the f_k become coupled. One can easily show that allowing K to depend on X leads to an infinite system of equations for the f_k which are coupled and each of these equations contain $\partial^n K/\partial X^n$, $n = 0, 1, \ldots, \infty$. Thus, it is clear that the dispersion model does not apply, in a predictable way at least, to flows in which u_1 and v_1 depend on X in an arbitrary way. It will be seen later, when examining steady flows in the velocity entrance region of circular tubes, that the dispersion model applies only when the entrance region constitutes a fairly small fraction of the total system under consideration so that the velocity field is independent of X in most of the region of interest.

When one is dealing with time dependent flows that develop from rest in tubes, the velocity distribution is well known (*4*) and is given by

$$u_1(\tau, y) - U(\tau) = \frac{1}{2} - y^2 + 16 \sum_{n=1}^{\infty} \frac{e^{-\alpha_n^2 N_{Sc}\tau}}{\alpha_n^4} \left\{ 1 - \frac{\alpha_n}{2} \frac{J_0(\alpha_n y)}{J_1(\alpha_n)} \right\} \quad (19)$$

where α_n are the roots of

$$J_0(\alpha_n) = 0 \quad (20)$$

In this case one can easily show, by solving Equation (11*a*) with the aid of the Duhamel theorem, that f_1 is given by

$$f_1 = \sum_{n=1}^{\infty} \frac{4}{\gamma_n^4} \left(1 - e^{-\gamma_n^2 \tau} \right) \frac{J_0(\gamma_n y)}{J_0(\gamma_n)} - 16 \sum_{n=1}^{\infty} \frac{J_0(\gamma_n y)}{J_0(\gamma_n)} \sum_{q=1}^{\infty} \frac{\left[e^{-\alpha_q^2 N_{Sc}\tau} - e^{-\gamma_n^2 \tau} \right]}{\alpha_q^2 (\alpha_q^2 - \gamma_n^2)^2 (\alpha_q^2 N_{Sc} - \gamma_n^2)} \quad (21)$$

Consequently, from Equation (18)

$$K(\tau) = \frac{1}{N_{Pe}^2} + 16 \sum_{q=1}^{\infty} \frac{\left(1 - e^{-\gamma_q^2 \tau}\right)}{\gamma_q^6} + 64 \sum_{n=1}^{\infty} \frac{e^{-\alpha_n^2 \tau}}{\alpha_n^2} \sum_{q=1}^{\infty} \frac{\left(1 - e^{-\gamma_q^2 \tau}\right)}{\gamma_q^4 (\alpha_n^2 - \gamma_q^2)} - 64 \sum_{n=1}^{\infty} \frac{1}{\gamma_n^2} \sum_{q=1}^{\infty} \frac{\left[e^{-\alpha_q^2 N_{Sc}\tau} - e^{-\gamma_n^2 \tau} \right]}{\alpha_q^2 (\alpha_q^2 - \gamma_n^2)^2 (\alpha_q^2 N_{Sc} - \gamma_n^2)} + 256 \sum_{s=1}^{\infty} \frac{e^{-\alpha_s^2 N_{Sc}\tau}}{\alpha_s^2} \sum_{n=1}^{\infty} \frac{1}{\alpha_s^2 - \gamma_n^2} \sum_{q=1}^{\infty} \frac{e^{-\alpha_q^2 N_{Sc}\tau} - e^{-\gamma_n^2 \tau}}{\alpha_q^2 (\alpha_q^2 - \gamma_n^2)(\alpha_q^2 N_{Sc} - \gamma_n^2)} \quad (22)$$

with γ_n defined by

$$J_1(\gamma_n) = 0 \quad (23)$$

For the case of a slug of dimensionless initial length X_s dispersing in the velocity field given by Equation (19), one has as a solution to Equation (8):

$$\theta_m = \frac{1}{2} \operatorname{erf} \left[\frac{\frac{1}{2} X_s + X_1}{\sqrt{4\overline{K}\tau}} \right] + \frac{1}{2} \operatorname{erf} \left[\frac{\frac{1}{2} X_s - X_1}{\sqrt{4\overline{K}\tau}} \right] \quad (24)$$

where

$$\overline{K} = \frac{1}{\tau} \int_0^{\tau} K(\tau)\, d\tau \quad (25)$$

Equations (22) to (25) apply for all values of the Peclet number since axial molecular diffusion has been included in the analysis. If the flow is steady, Equation (22) reduces to

$$K_{s.s.} = \frac{1}{N_{Pe}^2} + \frac{1}{192}$$

RESULTS AND DISCUSSION

Velocity Entrance Region of a Tube

The velocity distribution results of Christiansen and Lemmon (*6*) were used in the finite difference solution for the constant physical property, steady state flow in the entrance region of a tube. In this case, the dispersion system depends on both the Reynolds number and the Schmidt number rather than just their product, the Peclet number, as it does in fully developed laminar systems. Consequently it is convenient to consider high and low Schmidt number systems separately. All calculations for the velocity entrance region were made for a step change in concentration at $X = 0$.

High Schmidt Number Region

For liquid systems, such as salt water where N_{Sc} is on the order of 550, and for laminar flows with $N_{Re} = 2{,}000$, it was found that the developing velocity profile has negligible effects on dispersion as can be seen from Figure 1. From Figure 1 it is clear that even for very low

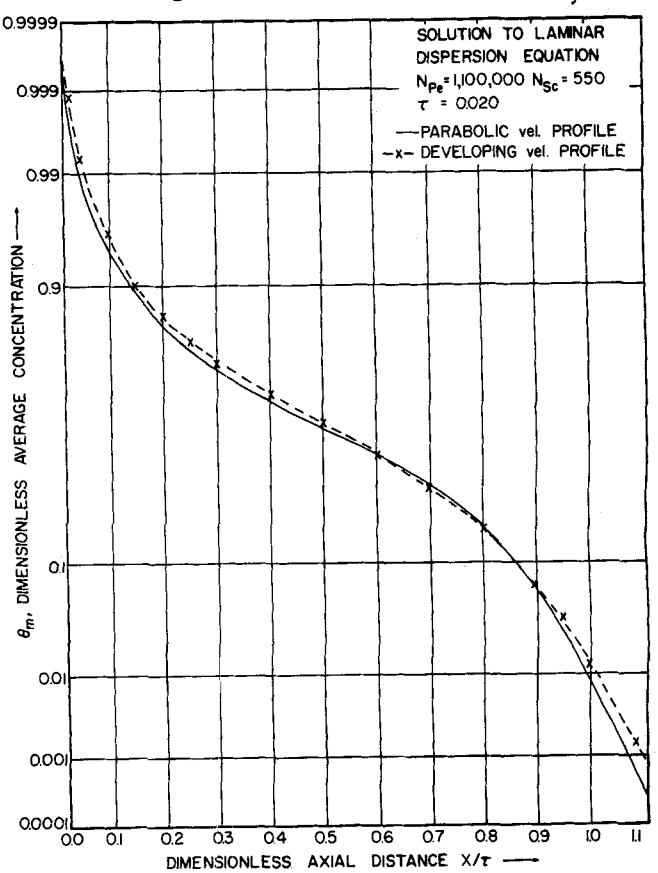

Fig. 1. Dispersion in fully developed flow and in entrance region flow for small τ. Comparison of finite difference solution of Equation (1) for Poiseuille flow with tube entrance region flow, N_{Sc} = 550 and τ = 0.020.

dimensionless times, $\tau = 0.020$, the two solutions, one with *parabolic velocity* profile and the other with the developing velocity profile, are the same. It is at these small times that one expects the effect of developing velocity profile to be the greatest and thus it follows that for all higher times the solutions will be identical, as was also verified.

This result is reasonable because at a Peclet number of 1.10×10^6, the velocity entrance region is relatively short and it comprises only a small fraction of the total length of the tube section in which dispersion is occurring. Thus the effect of the developing velocity profile is essentially negligible in all regions of practical interest. For example, it is known (*6*) that the entrance length for velocity is given as $x_{entrance}/R\,N_{Re} \simeq 0.12$. Consider then the case of very small dimensionless times, or τ values such as $\tau = 0.020$ when the dispersion takes place mainly by convection. In this case, for a very small dimensionless axial distance, say $X = x/R\,N_{Pe} = 0.002$, we find $x/R = 2{,}200$ while the velocity entrance length extends only up to

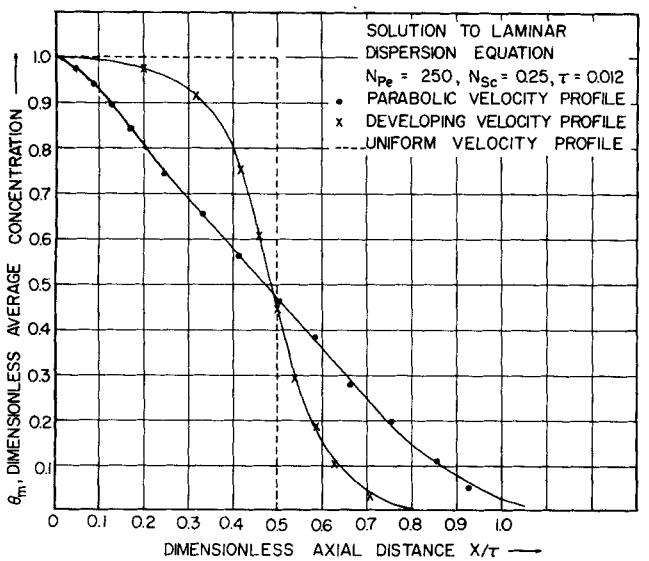

Fig. 2. Dispersion in tube entrance region fully developed and plug flows for small τ. Comparison of finite difference results for tube entrance region with the plug flow solution, for $N_{Pe} = 250$, $N_{Sc} = 0.25$ and $\tau = 0.012$.

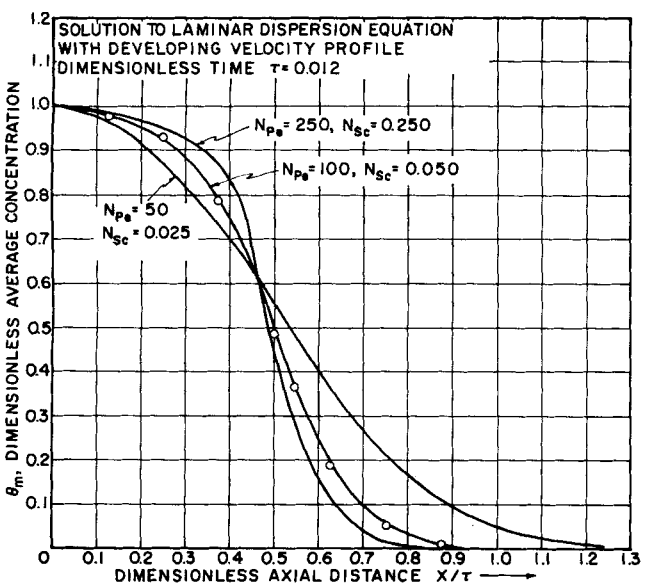

Fig. 3. Effect of N_{Sc} and N_{Pe} on tube entrance region results. Comparison of finite difference solution to Equation (1) with laminar developing velocity for $N_{Sc} = 0.50$, 0.050, and 0.025 at $\tau = 0.012$.

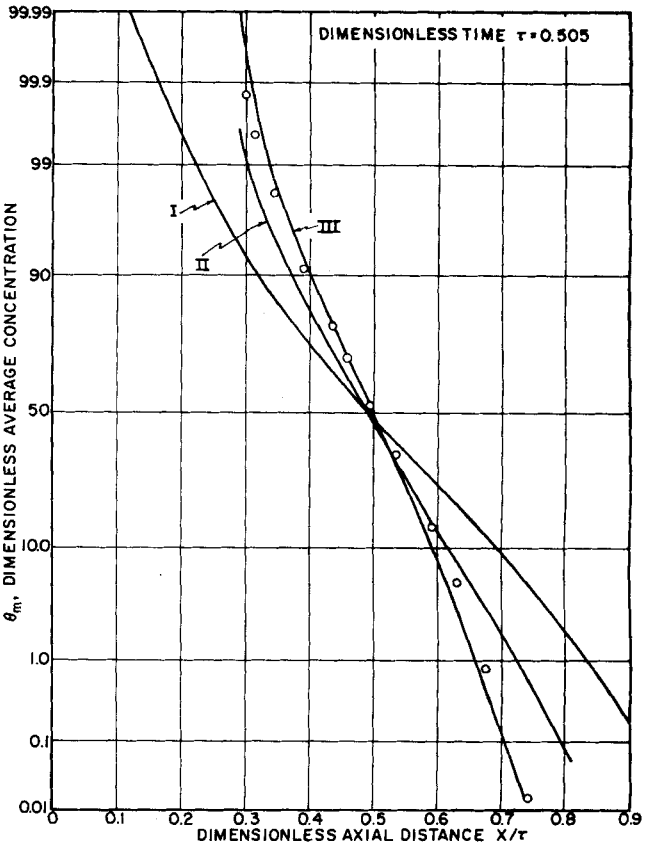

Fig. 4. Finite difference solutions of Equation (1) with fully developed and tube entrance region flows for $\tau = 0.505$. Curve I: fully developed parabolic velocity profile, $N_{Pe} = 50$; Curve II: entrance region developing velocity profile, $N_{Pe} = 250$, $N_{Sc} = 0.25$; Curve III: denotes solution with developing velocity profile for $N_{Pe} = 50$, $N_{Sc} = 0.025$; Circles, o, denotes solution with developing velocity profile for $N_{Pe} = 100$, $N_{Sc} = 0.05$.

$x/R = 240$. Hence, even the point $X = 0.002$ is too far away from the entrance region to be affected by the developing velocity profile.

Low Schmidt Number Region

In case of gaseous dispersion, where the Schmidt number is of the order 0.25 to 1.0 and for Reynolds number of say 1,000, it was found that the developing velocity profile makes a significant difference in the solution of the convective diffusion equation. For a small value of time of $\tau = 0.012$, Figure 2 shows a comparison of the solutions to the convective diffusion equation for $N_{Pe} = 250$ and $N_{Sc} = 0.25$ which were obtained by using parabolic, developing and uniform velocity profiles. It can be seen from the figure that the solution for the developing velocity profile is between the uniform and fully developed ones and that there is a significant effect of the developing velocity profile on the dispersion.

The reason for this is that in the case of low Schmidt number, the region of practical interest in which the dispersion takes place may be well within the velocity entrance region. For example, in the above case where $N_{Pe} = 250$ and $\tau = 0.012$, for axial distances of $X/\tau = 1.0$, which is about as far as the solute penetrates, the value of x/R is 3.0 while the velocity entrance region extends up to $x/R = 120$. In fact, it will take a rather long time, or high τ value, for the velocity entrance region to be a negligible fraction of the region in which dispersion is taking place.

As time increases the velocity field approximates the fully developed flow more closely. Consequently the average concentration distributions become more alike as was seen in Figure 1.

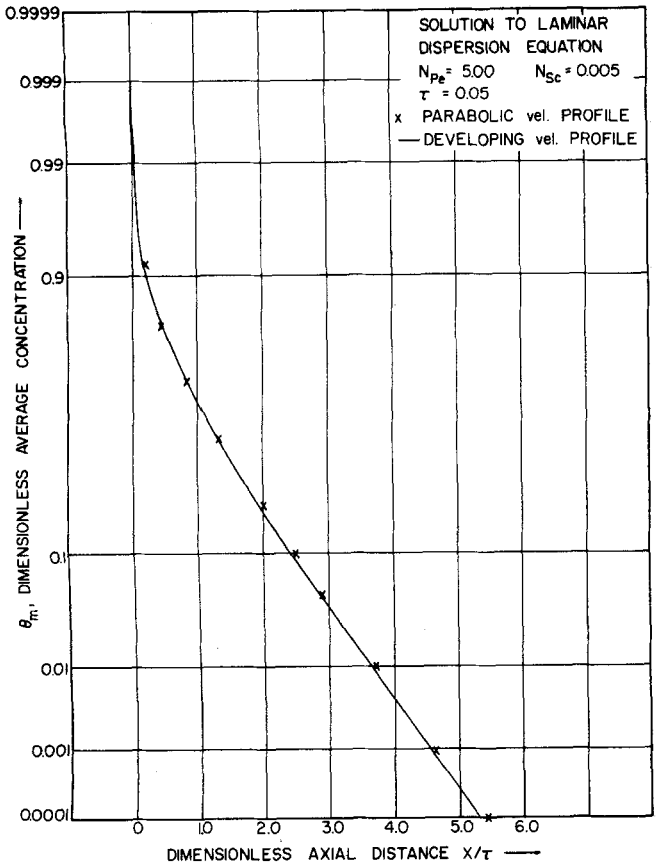

Fig. 5. Finite difference solution of Equation (1) with laminar developing and parabolic velocity profiles for N_{Pe} = 5.00, N_{Sc} = 0.005 and τ = 0.05.

As the Schmidt number decreases below 0.25, for the range of Reynolds numbers on the order of 2,000 or less, axial molecular diffusion starts to become significant. The effect of the axial molecular diffusion is to increase the overall extent of dispersion. This effect can be seen in Figure 3 where average concentration distribution curves are given for Schmidt numbers of 0.25, 0.05 and 0.025* at Reynolds numbers ranging from 1,000 to 2,000, and at a time τ = 0.012. For the curves shown the ratios of the velocity entrance lengths, to the lengths of the dispersion region are about 100 or greater and therefore, in all cases the velocity profile is essentially flat throughout the entire mixing zone and the difference among these three curves is caused largely by axial molecular diffusion.

From Figure 4 it can be seen that for higher values of τ the solution for N_{Sc} = 0.25 deviates less from the fully developed solution than do the solutions for N_{Sc} = 0.05 and 0.025. In these cases the ratio of the length of the velocity entrance region to the length of the dispersion mixing zone is on the order of 1, 5, and 10 for N_{Sc} equal 0.25, 0.05 and 0.025 respectively.

Figure 4 suggests, and plots at higher values of τ confirm, that the solutions tend to become error functions as time increases but with a dispersion coefficient less than that which would be obtained if the flow were fully developed. For example an expression which agrees reasonably well with the developing velocity profile numerical solution for τ = 1.345 is given by

$$\theta_m = \frac{1}{2}\operatorname{erfc}\left[\frac{X-\tau/2}{\sqrt{\frac{\tau}{e}+\frac{4\tau}{N_{Pe}^2}}}\right]$$

* The cases of 0.025 and 0.05 are best interpreted in terms of the dispersion of thermal energy rather than mass.

where e = 122. For fully developed flow e = 48, and thus it can be seen that the apparent dispersion coefficient is substantially smaller in the case where the velocity profile is developing over about 40% of the mixing zone. As $\tau \to \infty$ the region of developing velocity becomes a negligible fraction of the total distance X reached by the dispersing substance, and one would expect that solutions would become identical in each case as occurred with high Peclet numbers. Thus e will clearly be a function of τ and should tend to 48 for very large τ.

For extremely low Schmidt numbers of the order of N_{Sc} = 0.005 (these, as is the case also for N_{Sc} = 0.025 and 0.05, are more appropriate to thermal dispersion in a liquid metal flowing in an insulated pipe rather than mass dispersion) and for laminar flow with N_{Re} = 1,000, the Peclet number is small, N_{Pe} = 5, and at short times dispersion takes place by pure molecular diffusion. Consequently, the velocity profile, whether developing or fully developed does not play an important role in the overall dispersion process and the two solutions are identical as is seen in Figure 5. Even though dispersion does not take place beyond the velocity entrance region up to a τ on the order of 20, it was found that for moderately large τ, say τ = 2.2, the effect of axial molecular diffusion still predominates and the developing velocity profile is of little significance. This is seen in Figure 6 where at τ = 2.2, solutions for both the developing and parabolic velocity profile cases show good agreement with each other.

Time Dependent Velocity

It is easy to show by using Equation (19) that the velocity profile is very close to being fully developed when

$$\tau \simeq \frac{0.5}{N_{Sc}}$$

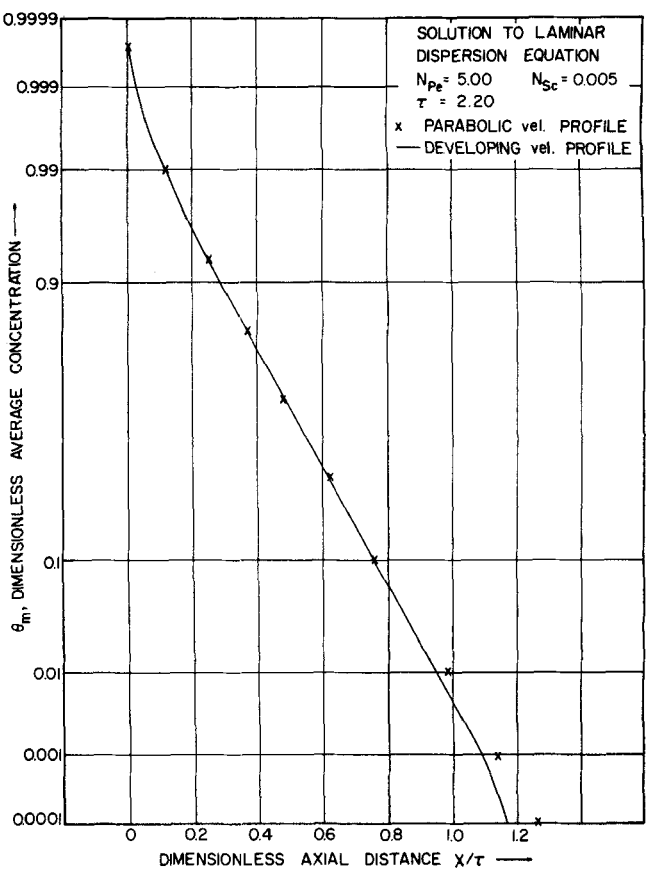

Fig. 6. Finite difference solutions of Equation (1) with laminar developing and parabolic velocity profiles for N_{Pe} = 5.0, N_{Sc} = 0.005 and τ = 2.20.

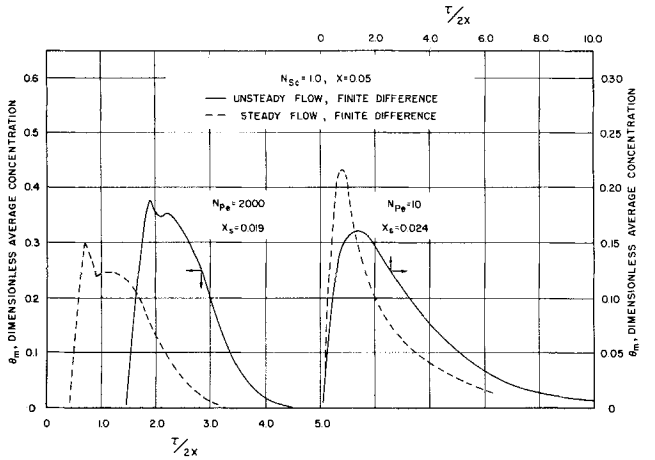

Fig. 7. Concentration distributions as function of τ at $X = 0.05$ for steady and unsteady flow and $N_{Pe} = 2{,}000, 10$.

Therefore the dimensionless time required for this to occur is inversely proportional to N_{Sc} so that the effect of the transient part of the velocity field is greater in low Schmidt number systems. For this reason finite difference calculations were carried out for N_{Sc} equal unity which would be in the range of gaseous flows.

The largest differences between dispersion with steady state (S.S.) and time dependent velocity fields (T.D.) will naturally occur close to the entrance of the system where all significant changes in concentration happen at relatively small values of τ. It can be seen in Figure 7 that the concentration distribution in the T.D. case is displaced to the right of the S.S. curve significantly more when $N_{Pe} = 2{,}000$ than when $N_{Pe} = 10$. This occurs because convection is the only significant axial transport mechanism for high Peclet numbers whereas molecular diffusion is important when $N_{Pe} = 10$.

A comparison of the finite difference and dispersion model results given by Equation (24) is shown in Figures 8 and 9 for $X = 0.5$ and 1.0. It is seen that the peak mean for the S.S. results occurs at $\tau/2X \leq 1.0$ whereas the peak mean of the T.D. results occurs at $\tau/2X > 1.0$. This happens because the mean residence time is greater in the T.D. case. It is interesting to note that the agreement between the finite difference solutions and Equation (24) is somewhat better at $N_{Pe} = 10$ than at $N_{Pe} = 2{,}000$.

In an experimental investigation one would determine a C curve by measuring the mean concentration as a function of time at a particular location downstream of the position of the slug at $t = 0$. If the experimental results are to be interpreted in terms of the dispersion model then

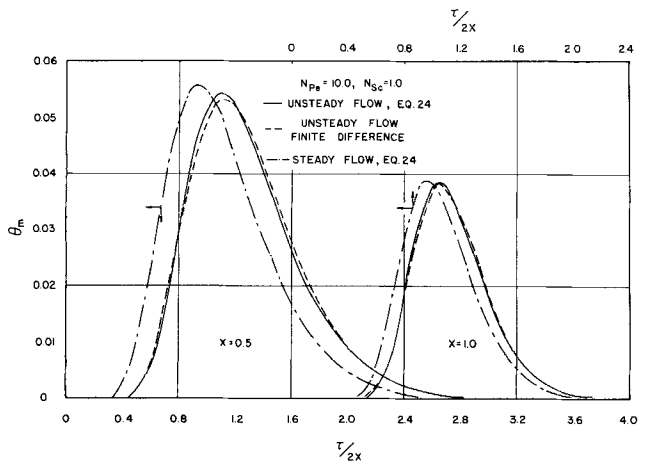

Fig. 8. Comparison of Equations (24) for unsteady and steady flow with finite difference solutions for unsteady flow with $N_{Pe} = 10$.

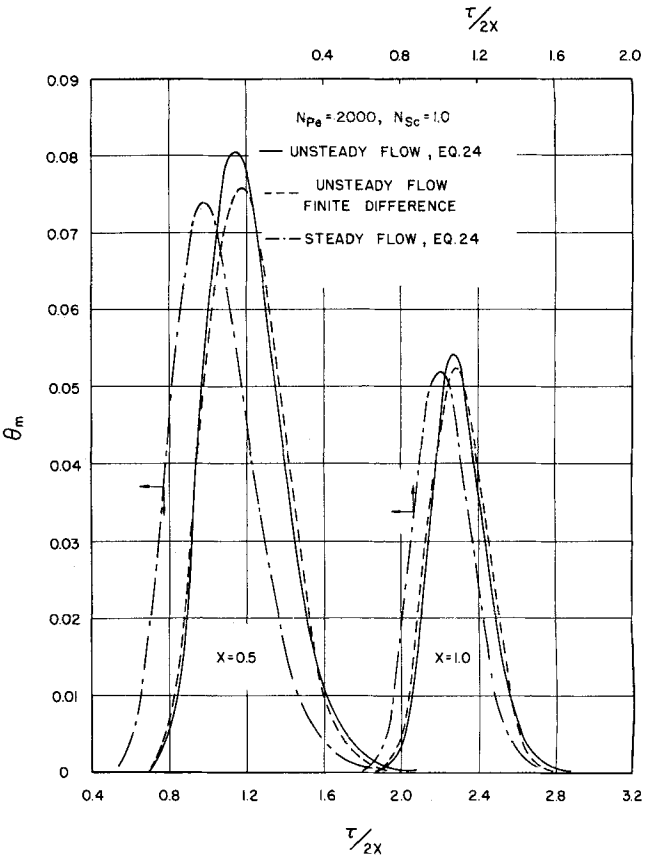

Fig. 9. Comparison of Equations (24) for unsteady and steady flow with finite difference solutions for unsteady flow with $N_{Pe} = 2{,}000$.

it is necessary for the observation point to be sufficiently far downstream for Equation (24) to apply. We can estimate the distance necessary by comparing Equation (24) with the finite difference results. If one sets 5% as the maximum allowable difference between Equation (24) and the finite difference results as the criterion for the dispersion model to apply, then it is necessary to position the observation point at approximately $X > 0.6$ for $N_{Pe} = 2{,}000$ and $X > 0.15$ for $N_{Pe} = 10$. Since the results are independent of Peclet number when $N_{Pe} > 100$, it follows that $X > 0.6$ should be satisfactory in most cases of practical interest.

One may wish to measure the average concentration as a function of axial distance at various values of time. In this case, minimum values of τ necessary for Equation (24) to be valid are about the same with steady or unsteady flow and are approximately $\tau = 0.6$ and 0.3 at $N_{Pe} = 2{,}000$ and $N_{Pe} = 10$ respectively. As mentioned

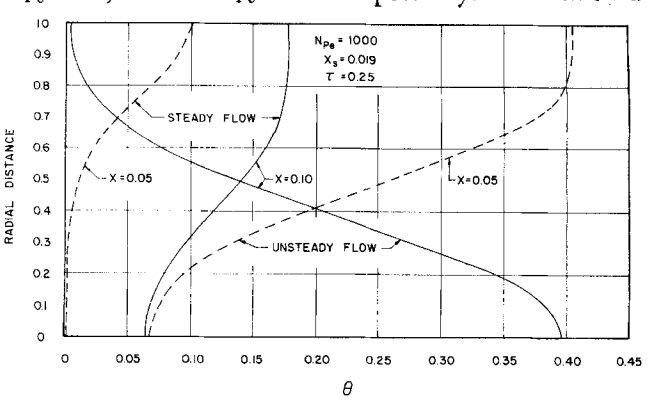

Fig. 10. Comparison of local concentration distributions in steady and unsteady flows.

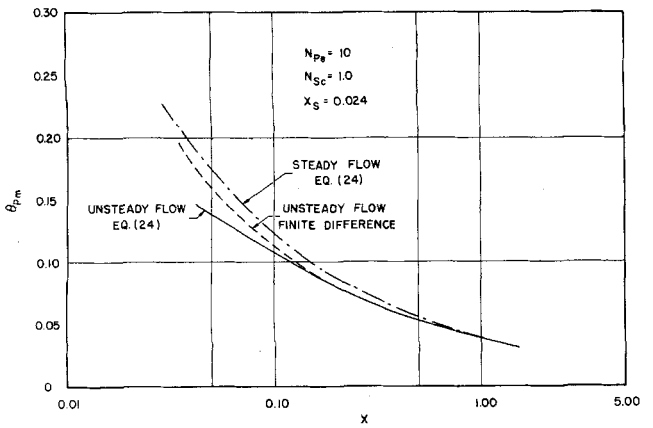

Fig. 11. Comparison of peak mean concentration distributions for steady and unsteady flow at $N_{Pe} = 10$.

above, the results are independent of Peclet number when $N_{Pe} > 100$ and therefore $\tau = 0.6$ should be satisfactory in practice.

Although average concentration distributions in T.D. and S.S. flows differ significantly, the differences are not really dramatic. In contrast local distributions in these cases may be very striking. This is demonstrated in Figure 10.

Because one may determine conveniently the dispersion coefficient by measuring peak mean concentrations it is interesting to compare the peak mean concentration distribution as a function of X for both Peclet numbers studied as shown in Figures 11 and 12. With high Peclet numbers, the peak mean concentrations for the T.D. case are higher than those for the S.S. flows; this occurs because the dispersive effect of axial convection, which is the only mechanism contributing to axial dispersion, is less in the T.D. case. For low Peclet number flows molecular diffusion contributes to axial dispersion and the longer average residence time characteristic of T.D. flows enables this mechanism to overcompensate for the decrease in the axial convection effect. Therefore the peak mean concentration is lower in low Peclet number T.D. than S.S. flows.

Previously it was mentioned that it is necessary for the observation point to be at a sufficiently large value of X in order for Equation (24) to be valid. One can get a reasonable estimate of the maximum error involved in using Equation (24) by the comparison with finite difference results as given in Figures 11 and 12. This is so because the differences between the peak mean concentrations given by Equation (24) and the finite difference results are reasonably close to the maximum differences.

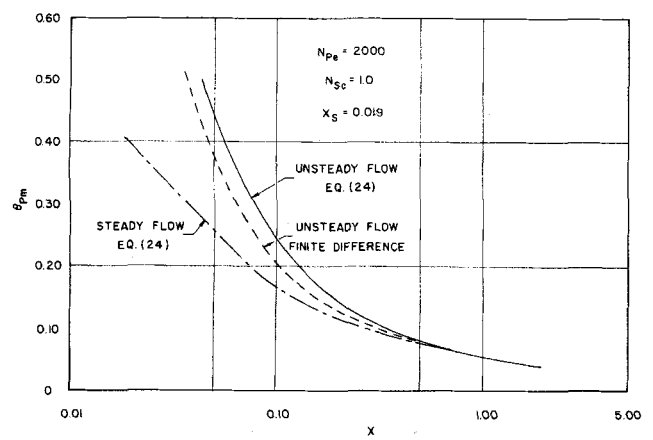

Fig. 12. Comparison of peak mean concentration distributions for steady and unsteady flow at $N_{Pe} = 2{,}000$.

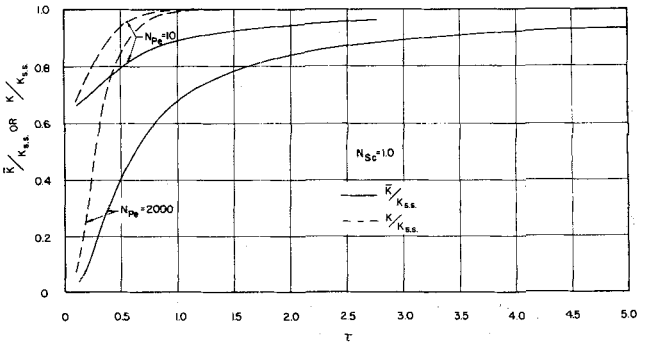

Fig. 13. Ratio of dispersion coefficients, for flows starting from rest, K and $\bar{K}$, defined by Equations (22) and (25) to the steady flow value, $K_{s.s.}$

From Equation (22), it is seen that the parametric dependence of K can be denoted as

$$K = K(\tau, N_{Sc}, N_{Pe})$$

The dependence of K on τ is shown graphically in Figure 13 in terms of $K/K_{s.s.}$ and $\bar{K}/K_{s.s.}$. It is seen that $K/K_{s.s.}$ approaches unity rapidly but $\bar{K}/K_{s.s.}$ changes much more slowly.

CONCLUDING REMARKS

The practical effects of developing velocity profiles on dispersion are most pronounced for systems with Schmidt numbers on the order of unity or less. This is true both when the velocity entrance region comprises a significant fraction of the mixing zone and when the velocity field develops from rest. The velocity entrance region is most likely to be important in experiments involving a step change in concentration at the inlet of the system while the velocity field which develops from rest is likely to be associated with slug inputs.

The dispersion coefficient is smaller when the velocity entrance constitutes a significant fraction of the mixing zone than when the velocity profile is fully developed throughout the system. When the velocity profile develops from rest the dispersion coefficient is also smaller than in the fully developed case. This occurs because it is the nonuniformity in the local velocity distribution across the flow and hence the nonuniformity in the local residence time distribution, which enhances the dispersion coefficient. In entrance region flows, or flows which develop from rest, axial distance in the former or time in the latter is required for the velocity field to achieve its maximum peakedness.

The time dependent dispersion coefficient enters the solution of the convective diffusion equation without causing difficulty as a time dependent eigenvalue when the velocity field is a function of time. However, at least in the dispersion model solution developed here, a dispersion coefficient which depends on axial position is inadmissible.

ACKNOWLEDGMENT

This work was sponsored in part by the Office of Saline Water, U.S. Department of Interior. The numerical calculations were done at the Computing Center of Clarkson College and at the Computing Center of the State University of New York at Buffalo. The Computing Center at the State University of New York at Buffalo is partially supported by NIH Grant FR-00126 and NSF Grant GP-5675.

NOTATION

C = local point concentration

C_R = reference concentration: Slug concentration at $t = 0$ for slug stimulus. Concentration at $X = 0$ for flow in tube velocity entrance region

D = molecular diffusion coefficient
D_r = total radial diffusion coefficient, $D_r = D + \epsilon_r$
D_x = total axial diffusion coefficient, $D_x = D + \epsilon_x$
D_1 = dimensionless total radial diffusion coefficient, D_r/D
D_2 = dimensionless total axial diffusion coefficient, D_x/D
f_k = functions defined by Equations (6) and (11)
F = function defined by Equation (12)
G = function defined by Equation (14)
J_0 = zero order Bessel function of first kind
J_1 = first order Bessel function of first kind
K = dispersion coefficient defined by Equation (8)
$\overline{K}$ = time average dispersion coefficient defined by Equation (25)
N_{Pe} = Peclet number, $U_R R/D$
N_{Sc} = ν/D
r = radial coordinate
R = tube radius
t = time
u = axial velocity
u_1 = u/U_R
U_R = reference velocity, $2U(\infty)$ where $U(\infty)$ is the bulk average velocity corresponding to fully developed laminar flow
v = radial velocity coordinate
v_1 = v/U_R
x = axial distance
X = $x/R\ N_{Pe}$
x_s = length of slug at $t = 0$
X_s = x_s/RN_{Pe}
y = r/R
α_n = roots of $J_0(\alpha_n) = 0$
γ_n = roots of $J_1(\alpha_n) = 0$
ϵ = eddy diffusion function
θ = dimensionless local concentration, C/C_R
θ_m = dimensionless average concentration
λ = auxilliary parameter replacing τ when applying Duhamel theorem
ν = kinematic viscosity
τ = dimensionless time, tD/R^2
σ = auxilliary parameter replacing X when applying Duhamel theorem

LITERATURE CITED

1. Ananthakrishnan, V., W. N. Gill, and A. J. Barduhn, *AIChE J.*, **11**, 1063 (1965).
2. Aris, Rutherford, *Proc. Roy. Soc. (London)*, **252A**, 538 (1959).
3. Bailey, H. R., and W. B. Gogarty, *ibid.*, **259A**, 352 (1962).
4. Bird, R. B., W. E. Stewart, and E. N. Lightfoot, "Transport Phenomena," John Wiley, New York (1960).
5. Carrier, G. F., *Quart. Appl. Math.*, **14**, 108 (1956).
6. Christiansen, E. B., and H. E. Lemmon, *AIChE J.*, **11**, 995, (1965).
7. Gill, W. N., *Proc. Roy. Soc. (London)*, **298A**, 335 (1967).
8. ———, and V. Ananthakrishnan, *AIChE J.*, **13**, 801 (1967).
9. Gill, W. N., *Chem. Eng. Sci.*, **22**, 1013 (1967).
10. Philip, J. R., *Australian J. Phys.*, **16**, 287 (1963).
11. Taylor, G. I., *Proc. Roy. Soc., (London)*, **219A**, 186 (1953).
12. Fan, L. T., and C. L. Hwang, *Kansas State Univ., Bull., Spec. Rep.*, 67, **50**, No. 3 (1966).
13. Lighthill, M. J., *J. Inst. Math. Its Appl.*, **2**, 97 (1966).

Manuscript received September 11, 1967; revision received December 19, 1967; paper accepted January 8, 1968.

Stability of Numerical Integration Techniques

G. P. DISTEFANO

Monsanto Company, St. Louis, Missouri

This paper presents the cause of instabilities which arise during the numerical solution of ordinary differential equations. By using the numerical integration routines presently available, one actually approximates the differential equation by a difference equation. If the difference equation is of a higher order than the original differential equation, the approximate solution contains extraneous solutions which are not at all related to the true solution. It is the behavior of these extraneous solutions that one is usually concerned with in a stability analysis.

Also presented is a procedure for obtaining a bound on the largest allowable integration step size for a class of chemical engineering problems. A detailed explanation of the procedure is illustrated for unsteady state distillation calculations.

The purpose of this paper is to present a clear, concise discussion of the main causes of instabilities which arise during the numerical integration of ordinary differential equations on a digital computer. Ordinary differential equations are an integral part of chemical engineering calculations in such basic areas as chemcial kinetic studies, transient distillation, heat transfer, etc. The complexity of such systems vary from a single equation to a system of several hundred simultaneous differential equations. In practice, these equations are usually highly nonlinear, and one must resort to numerical techniques in order to obtain a solution.

Two main problems arise in the numerical solution of differential equations, truncation error and numerical instability. Truncation error usually lends itself nicely to rigorous error analysis, and procedures are available to contain truncation error within some prescribed limits. Numerical instability, on the other hand, is more complex, and only in the recent literature has there been any attempt at a rigorous mathematical analysis.

By using the numerical integration routines presently available, one actually approximates a differential equation by a difference equation which is solved in a step-by-step or marching fashion.

STABILITY

It is important to begin this paper with a clear definition between convergence and stability of finite difference techniques. By convergence one means that the finite difference solution approaches the true solution as the

G. P. Distefano is now with Electronic Associates, Inc. Princeton, New Jersey.